AUTOMATIC GRAIN CLASSIFICATION CONSIDERATIONS

by

DARSHAN KUMAR SINGLA

B. E. (Electrical), Thapar Engineering College
Patiala, India, 1968

A MASTER'S REPORT

submitted in partial fulfillment of the

requirements for the degree

MASTER OF SCIENCE

Department of Electrical Engineering

KANSAS STATE UNIVERSITY
Manhattan, Kansas

1972

Approved by:

Nasir Ahmed
Major Professor

TABLE OF CONTENTS

CHAPTER I

INTRODUCTION

1.1 Introductory Remarks

All forms of grain sample analysis include a determination of the amount of material in the sample which is not the grain being analysed. The methods which are presently employed make use of various sieves of appropriate sizes, followed by a manual hand-picking of the remainder. The hand-picking process is carried out separately since it is both tedious and time consuming. To this end, it is desirable to automate the hand-picking part of the analysis by an appropriate scheme. Such a scheme should possess the capability of distinguishing between a variety of grains which includes wheat, barley, oats, rye, soybeans and milo.

The purpose of this report is two-fold. First it presents a review of the pertinent literature. Second, it extends an initial feasibility study which was reported recently by Vyas*. The approach entertained by Vyas was based on pattern recognition techniques. The types of grains considered were:

(1) corn, (2) wheat, (3) barley, (4) oats and (5) milo.

In this study, two additional types of grain namely rye and soybeans are also considered. Again, the study by Vyas was restricted to linear classifiers. In this report, quadratic classifiers are also considered.

---

*A. H. Vyas, "A Pattern Recognition Approach to Grain Sample Analysis", Master of Science report, Electrical Engineering Department, Kansas State University, Manhattan, Kansas.

1.2 General Remarks Pertaining to Pattern Recognition Problems

The basic ideas associated with pattern recognition problems are best introduced by referring to Figure 1-1.

The signal acquisition stage acquires a set of signals from each of the classes which are to be classified. The signals acquired may be one-dimensional or multi-dimensional.

The output of the signal acquisition stage is denoted by C_i, $i=1,2,\ldots,K$, where C_i represents the i^{th} class, each of which consists of N_i signals. The j^{th} signal belonging to class i is denoted by x_{ij}. Thus for each i, j varies from 1 to N_i.

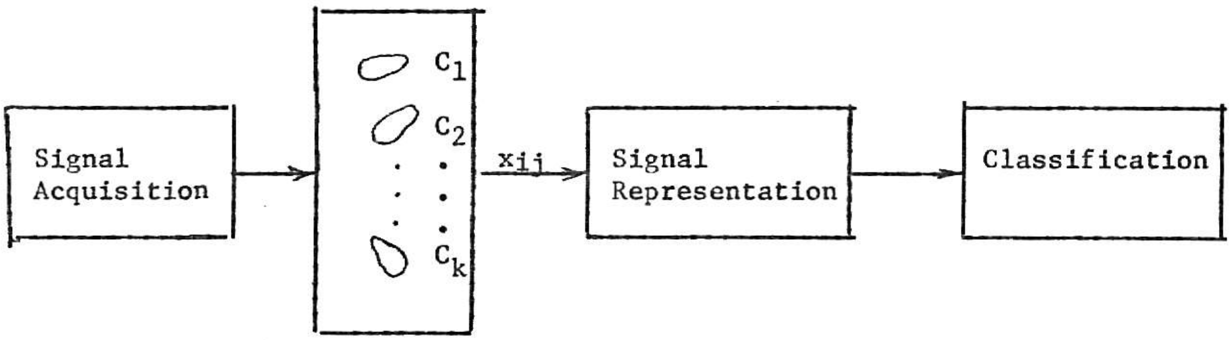

Figure 1.1 Block diagrams representation of a pattern recognition problem.

Consider a typical signal x_{ij} which is fed into a signal representation stage as shown in Figure 1-1. The role of the signal representation stage is to seek some "measurements", "features" or "attributes" which will help discriminate a signal x_{lj} from another signal x_{mj}, where $l \neq m$. The output of this stage corresponding to the input x_{ij} is denoted by P_{ij} which may be in the form of a finite n-dimensional vector or a finite multi-dimensional array. This P_{ij} is generally referred to as a pattern corresponding to the signal x_{ij}.

The classification stage in Figure 1-1 is a device which is trained to recognize a set of patterns $\{P_{ij}\}$. Consequently the set of patterns $\{P_{ij}\}$ whose classification is a known apriori is referred to as the training set. Once the classifier has been trained using the training set, it is conceivable that it will make errors while classifying patterns not belonging to the training set. There is a large number of training procedures available in the literature*. The procedure best suited for a specific application is generally dictated by the nature of the signal representation stage.

In conclusion, it is remarked that although the signal representation stage in Figure 1-1 plays a crucial role with respect to the overall system complexity and performance, very little theory is available which enables one to select the "best" measurements or features to represent the set of signals $\{x_{ij}\}$. Feature selection techniques vary from one pattern recognition problem to another. Some aspects of signal representation for the problem are briefly considered in the following section.

1.3 Signal Representation for Grain Classification

The signal representation technique used in this study is simple in that it concerns only the size and shape of a given kernel. Consider a black and white image of a grain kernel as shown in Figure 1-2.

The image frame in Figure 1-2 is devided into an (32x32) array. Again, each element of this array which contains the kernel is represented by a

---

*For an excellent summary, see "A Survey of Pattern Recognition", by W. G. Wee, IEEE Proc. of the Seventh Symposium on Adaptive Processing, December 1968, pp. 2-E-13.

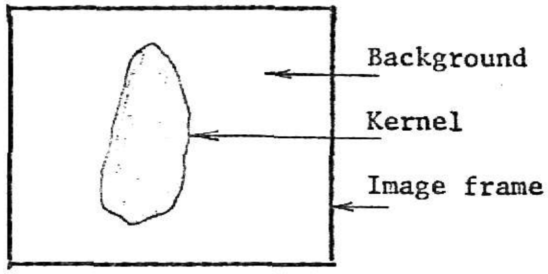

Figure 1-2 Black and White Image of a Kernel

"one" while the other elements are represented by "zeroes". An example of the coded image which results by this process is shown in Figure 1-3. Information pertaining to the size and shape of this image frame is extracted by means of a two-dimensional spectral analysis. The transform used for spectral analysis is analogous to the familiar Discrete Fourier Transform and is called the Walsh Hadamard or BIFORE (Binary Fourier Representation) transform. A brief introduction concerned with two-dimensional BIFORE transform is provided in Chapter III.

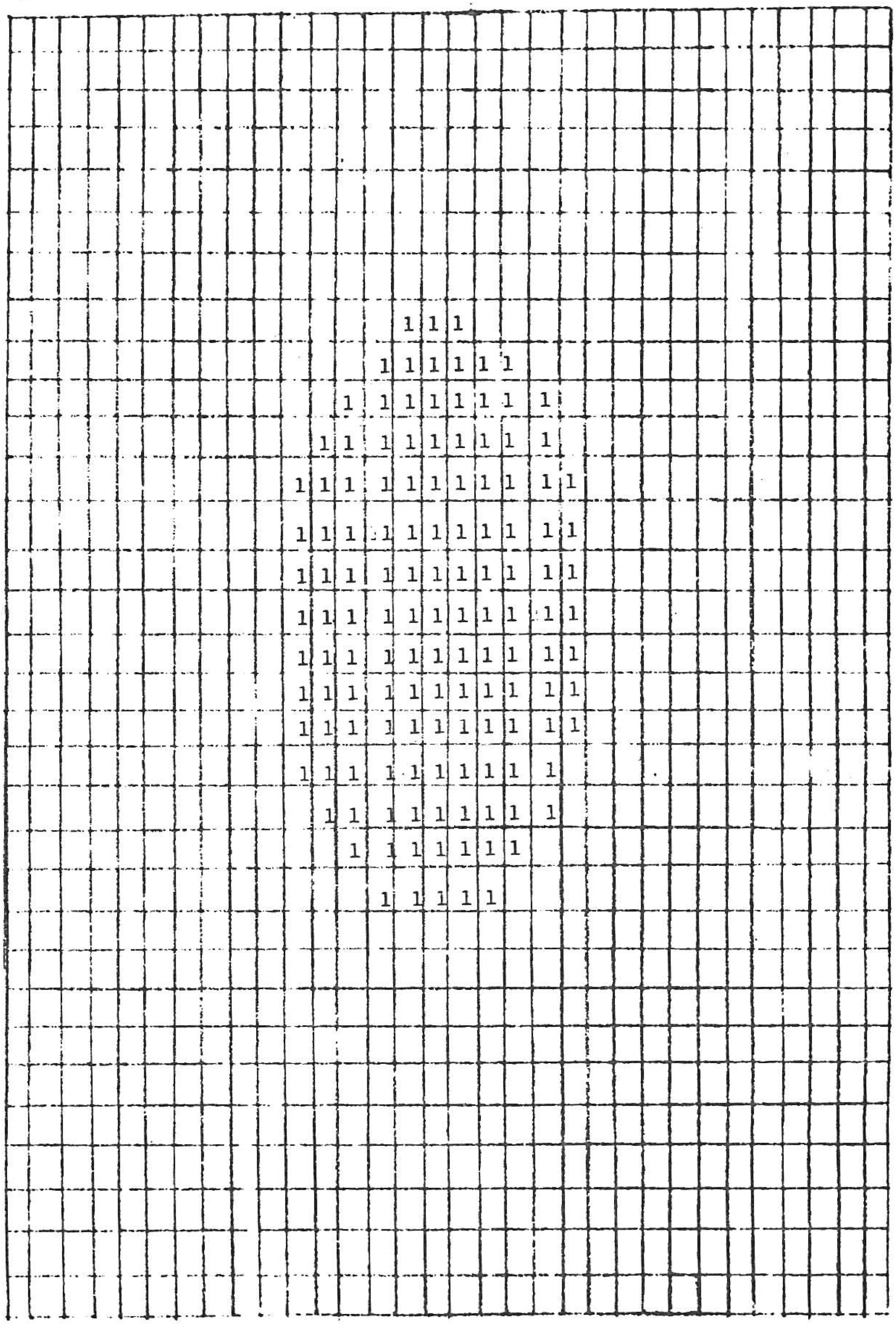

Figure 1-3. Typical output from microfilm reader.

(Blank elements of the array consist of zeros).

CHAPTER II

REVIEW OF THE LITERATURE

2.1 Introduction

A review of the literature published in the past decade shows that the only research effort besides that by Vyas [9] is one which was initiated in 1971 by Edison and Brogan [1]. This study is in progress at the present time. Two progress reports have been written, a summary of which is presented in what follows.

2.2 The Edison - Brogan Approach [1]

<u>Data Acquisition</u>

Basically, six categories or classes C_j, j=1,2,....,6 of grain were considered. These were the following:

(1) Corn

(2) Wheat

(3) Soybeans

(4) Oats

(5) Barley

(6) Rye

Physical measurements of length, width, height and projected area were made for 1000 kernels each of Wheat, Oats, Soybeans, Corn, Barley and Rye. <u>Ten</u> varieties of each kind were included except for Rye where only <u>seven</u> varieties were used as shown in Table 2-1.

A semi-automatic measuring system was assembled to obtain size data on grain samples. The system was utilized to measure the length, width, height

Table 2-1

List of Grain Varieties

Corn	Oats	Barley
Ia 4542 LR	Kata	Princes
Nebr 807	Jaycee	Dixon
NC + 50 LF	Pettis	Primas II
Nebr 501 D	Santee	Larker
Nebr 708	Neal	Otis
Nebr 611	Burnett	Trebi
NC + 53 MR	Garry	Liberty
NC + 11 SC MR	MO - 205	Kearney
NC + GO LF	Russell	Chase
Nebr 808	Garland	Custer

Soybeans	Wheat	Rye
Clark 63	Trapper	Elbon
Hawkeye	Trader	Cougar
SRF 300	Gage	Dakold
Kent	Scout 66	Pearl
Buson	Guide	Elbon
Cutler	Chanute	Frontier
Corsay	Lancer	Elk
Amsay	Scoutland	
Calland	Centurk	
Wayne	Satanta	

and projected area of a kernel and to record this data on punched paper tape for computer processing. This recording of the data was done using a analog-to-digital convertor by sampling a d.c. voltage which was proportional to the measurement. The sampled value was recorded on punched paper tape under control of a foot-actuated switch. This measuring process made it possible to obtain area and dimensional data on 100 kernels in less than 1 hour. The accuracy of the area measurement is ±0.003 square inches and for the linear measurements is about ±0.006 inches.

Several statistics were computed. Those that are pertinent to the present study are listed in Appendix 2-1.

Data Utilization

Three parameters, namely area, the ratio length / width and the ratio length / depth were used. This identification algorithm utilised a learning technique. The algorithm was based upon the assumption that all grains do not have equal probability of occurring in a particular sample. A "learning parameter" α was defined which changes the probability of occurrence of each grain as more information is gathered during a given run.

Let A, L, D, and W denote the area, length, depth and width of a kernel. Again, let the parameters A, L/D and L/W be denoted by a 3-dimensional measurement vector $\underline{m}$, where

$$\underline{m} = \begin{bmatrix} m_1 \\ m_2 \\ m_3 \end{bmatrix} \qquad (2\text{-}1)$$

where m_1=A, m_2=L/D and m_3=L/W. The mean values of $\underline{m}$ for each of the six categories C_j, j=1,2,...,6 are designated q_i, i=1,2,...,6.

Clearly, $\underline{m}$ in (2-1) can be looked upon as a random vector. It was assumed that the probability function $P(\underline{m}/C_j)$ associated with category C_j was Gaussian. That is

$$P(\underline{m}/C_j) = K\, e^{-\frac{1}{2}\, \underline{e}_j^T Q_j^{-1} \underline{e}_j}, \quad j=1,2,\ldots,6 \qquad (2\text{-}2)$$

where $K = \dfrac{1}{(2\pi)^{3/2} |Q_j|^{1/2}}$

$\underline{e}_j = \underline{m} - q_j$ $\underline{e}_j^T$ denotes the transpose of $\underline{e}_j$

and

Q_j is the (3x3) covariance matrix of category C_j while $|Q_j|$ denotes its determinant.

The covariance matrix Q_j in (2-2) was estimated using the experimental data collected in the data acquisition stage.

When all classes are equally likely to be present in the sample population maximizing this conditional probability function is equivalent to maximizing the probability that random measurement $\underline{m}$ really came from category C_j. However, the occurrence of a given category is also a random phenomenon, with a discrete probability distribution. If each of the six categories is equally likely, then $P(C_j) = 1/6$. This may be an appropriate assumption initially, but as more and more samples are investigated, additional knowledge is accumulated. For example, it may become apparent, after observing 10 straight samples of Rye, that the probability of occurrence of Rye is much higher than 1/6 for that particular population. What one should do is assign each sample to the category which results in the maximum probability that the random variable $\underline{m}$ belongs to category C_j, given all accumulated information. That is one must maximize

$$P(\underline{m},\ C_j|\underline{m}) = P(C_j|\underline{m}) \tag{2-3}$$

where P(E) denotes the probability of the event E.

Using Baye's rule, $P(\underline{m},\ C_j)$ can be written as

$$P(C_j,\ \underline{m}) = P(C_j|\underline{m})\ P(\underline{m}) = P(\underline{m}|C_j)\ P(C_j) \tag{2-4}$$

Thus

$$P(C_j|\underline{m}) = \frac{P(\underline{m}|C_j)\ P(C_j)}{P(\underline{m})} \tag{2-5}$$

where

$$P(\underline{m}) = \sum_{i=1}^{6} P(C_i|\underline{m}) = \sum_{i=1}^{6} P(\underline{m}|C_i)\ P(C_i)$$

Finally

$$P(C_j|\underline{m}) = \frac{P(\underline{m}|C_j)\ P(C_j)}{\sum_{i=1}^{6} P(\underline{m}|C_i)\ P(C_i)} \tag{2-6}$$

where

$P(\underline{m}|C_j)$ is given by (2-2).

Thus using the measurement vector $\underline{m}$ corresponding to a kernel which was to be classified as belonging to one of the categories C_j, $j=1,2,\ldots,6$, the decision process was carried out sequentially as follows:

(1) Assign apriori probabilities to each category i.e $P(C_j) = 1/6$ for example.

(2) Obtain measurements of $\underline{m}$ for a given sample and compute $P(\underline{m}|C_j)$ for $j=1,2,\ldots,6$ using Eq. (2-2).

(3) Compute the total probability for this particular $\underline{m}$ by summing over all six categories,

$$\sum_{i=1}^{6} P(\underline{m}|C_i)\ P(C_i)$$

(4) Form the six ratios $P(C_j|\underline{m})$ according to Eq. (2-6).

(5) Assign $\underline{m}$ to that category j for which $P(C_j|\underline{m})$ is largest.

(6) Based on the current sample $\underline{m}$, the a posteriori probability that C_j is present in the population is, by definition, the quantity computed in Eq. (2-6). However, the new $P(C_j)$ to be used with the next sample, is taken as a weighted average of the old probability (based on apriori estimates and all past data) and the posteriori probability.

$$P(C_j)_{new} = \alpha\, P(C_j)_{old} + (1-\alpha)\, P(C_j|\underline{m}) \qquad (2\text{-}7)$$

The parameter α is a "learning parameter". If α=0, all the weight is placed on the most recent estimate. If α=1, all the weight is placed on apriori estimate and no learning occurs. The value α=1 corresponds to the previously reported results and an accuracy of 80 to 85% was obtained.

The above scheme is being investigated. For example, by resetting all categories to be equally likely after each group of 50 samples, and using α=0.5, the results in Table 2.1 were obtained.

Table 2.2

Category	errors | no. of samples
1. corn	0 | 150
2. wheat	36 | 1000
3. soybeans	0 | 200
4. oats	2 | 1000
5. barley	93 | 1000
6. rye	15 | 850

With respect to the Table 2-2, it is reported that in the wheat category, 31 of 36 errors occurred on 100 samples of Scout 66 wheat and 50 samples of Trader wheat. Again, in the barley category, 72 of the 93 errors occurred on 100 samples of Trebi barley. These results imply that it is extremely difficult to separate certain types of wheat and barley from other types of grain.

The above summary was obtained from two progress reports [1] pertaining to a study which is being continued. However, no major changes in the identification scheme is expected. An attempt will be made to make the "best value" for the learning parameter α in (2-7). Some optical data having to do with reflectance properties of different types of grain will be incorporated into the identification process, if it proves to be useful in reducing errors.

APPENDIX 2-1

Summary For 1000 Kernels of Corn

	Length	Width	Depth	Area	L/W	L/D
Mean	.47296	.32082	.20403	.11474	1.4924	2.4288
Standard Deviation	.061624	.030223	.040493	.015850	.27507	.64476

Covariance Matrix

	Length	Width	Depth	Area
Length	$.37975\text{x}10^{-2}$	$-.68995\text{x}10^{-3}$	$-.13501\text{x}10^{-2}$	$.64562\text{x}10^{-3}$
Width	$-.68995\text{x}10^{-3}$	$.91349\text{x}10^{-3}$	$.11001\text{x}10^{-3}$	$.10482\text{x}10^{-3}$
Depth	$-.13501\text{x}10^{-2}$	$.11001\text{x}10^{-3}$	$.16396\text{x}10^{-2}$	$-.32088\text{x}10^{-3}$
Area	$.64562\text{x}10^{-3}$	$.10482\text{x}10^{-3}$	$-.32088\text{x}10^{-3}$	$.25122\text{x}10^{-3}$

Summary For 1000 Kernels of Wheat

	Length	Width	Depth	Area	L/W	L/D
Mean	.23654	.10991	.099534	.018779	2.1736	2.4012
Standard Deviation	.01784	.013054	.011926	.0026173	.24188	.27427

Covariance Matrix

	Length	Width	Depth	Area
Length	$.31834\text{x}10^{-3}$	$.94983\text{x}10^{-4}$	$.76844\text{x}10^{-4}$	$.31225\text{x}10^{-4}$
Width	$.94983\text{x}10^{-4}$	$.17041\text{x}10^{-3}$	$.91380\text{x}10^{-4}$	$.25208\text{x}10^{-4}$
Depth	$.76844\text{x}10^{-4}$	$.91380\text{x}10^{-4}$	$.14223\text{x}10^{-3}$	$.17609\text{x}10^{-4}$
Area	$.31225\text{x}10^{-4}$	$.25208\text{x}10^{-4}$	$.17609\text{x}10^{-4}$	$.68503\text{x}10^{-5}$

APPENDIX 2-1 (continued)

Summary For 1000 Kernels of Soybeans

	Length	Width	Depth	Area	L/W	L/D
Mean	.28732	.25276	.21151	.051916	1.1402	1.3650
Standard Deviation	.027126	.021707	.020077	.0077072	.10834	.14362

Covariance Matrix

	Length	Width	Depth	Area
Length	$.73587 \times 10^{-3}$	$.24517 \times 10^{-3}$	$.21014 \times 10^{-3}$	$.16373 \times 10^{-3}$
Width	$.24517 \times 10^{-3}$	$.47121 \times 10^{-3}$	$.28920 \times 10^{-3}$	$.12070 \times 10^{-3}$
Depth	$.21014 \times 10^{-3}$	$.28920 \times 10^{-3}$	$.40311 \times 10^{-3}$	$.96131 \times 10^{-4}$
Area	$.16373 \times 10^{-3}$	$.12070 \times 10^{-3}$	$.96131 \times 10^{-4}$	$.59401 \times 10^{-4}$

Summary for 1000 Kernels of Oats

	Length	Width	Depth	Area	L/W	L/D
Mean	.42686	.10456	.079946	.031001	4.1254	5.4582
Standard Deviation	.066858	.014559	.013060	.0069298	.69964	1.1862

Covariance Matrix

	Length	Width	Depth	Area
Length	$.44700 \times 10^{-2}$	$.37456 \times 10^{-3}$	$.18833 \times 10^{-3}$	$.35167 \times 10^{-3}$
Width	$.37456 \times 10^{-3}$	$.21197 \times 10^{-3}$	$.10991 \times 10^{-3}$	$.75719 \times 10^{-4}$
Depth	$.18833 \times 10^{-3}$	$.10991 \times 10^{-3}$	$.17058 \times 10^{-3}$	$.41528 \times 10^{-4}$
Area	$.35167 \times 10^{-3}$	$.75719 \times 10^{-4}$	$.41528 \times 10^{-4}$	$.48022 \times 10^{-4}$

APPENDIX 2-1 (continued)

Summary for 1000 Kernels of Barley

	Length	Width	Depth	Area	L/W	L/D
Mean	.34533	.12407	.098683	.028413	2.8255	8.5730
Standard Deviation	.048295	.015670	.015548	.0046847	.53775	.69878

Covariance Matrix

	Length	Width	Depth	Area
Length	$.23324 \times 10^{-2}$	$.10932 \times 10^{-3}$	$.87966 \times 10^{-4}$	$.16251 \times 10^{-3}$
Width	$.10932 \times 10^{-3}$	$.24556 \times 10^{-3}$	$.31626 \times 10^{-4}$	$.37646 \times 10^{-4}$
Depth	$.87966 \times 10^{-4}$	$.31626 \times 10^{-4}$	$.24174 \times 10^{-3}$	$.21240 \times 10^{-4}$
Area	$.16251 \times 10^{-3}$	$.37646 \times 10^{-4}$	$.21240 \times 10^{-4}$	$.21946 \times 10^{-4}$

Summary For 1000 Kernels of Rye

	Length	Width	Depth	Area	L/W	L/D
Mean	.26217	.086631	.082740	.017688	3.0533	3.7997
Standard Deviation	.028599	.010500	.010051	.0028382	.37982	.42519

Covariance Matrix

	Length	Width	Depth	Area
Length	$.81794 \times 10^{-3}$	$.11483 \times 10^{-3}$	$.93622 \times 10^{-4}$	$.62497 \times 10^{-4}$
Width	$.11483 \times 10^{-3}$	$.11026 \times 10^{-3}$	$.62282 \times 10^{-4}$	$.20322 \times 10^{-4}$
Depth	$.93622 \times 10^{-4}$	$.62282 \times 10^{-4}$	$.10103 \times 10^{-3}$	$.15757 \times 10^{-4}$
Area	$.62497 \times 10^{-4}$	$.20322 \times 10^{-4}$	$.15757 \times 10^{-4}$	$.80557 \times 10^{-5}$

CHAPTER III

THE TWO DIMENSIONAL BIFORE TRANSFORM

3.1 Definition

The shape and size of a kernel are used as criteria to distinguish it from a kernel belonging to a different type of grain. Each kernel is coded in the form of a (32x32) array of zeros and ones and can be represented by a matrix as follows:

$$\left[\underline{f}(x_1,x_2)\right] = \begin{bmatrix} f(0,0) & f(0,1) & \cdots\cdots & f(0,N_2-1) \\ f(1,0) & f(1,1) & \cdots\cdots & f(1,N_2-1) \\ \cdot & \cdot & \cdot & \\ \cdot & \cdot & \cdot & \\ f(N_1-1,0) & f(N_1-1,1) & \cdots\cdots & f(N_1-1,N_2-1) \end{bmatrix} \qquad (3\text{-}1)$$

where [1] $N_1=N_2=32$ and each of the $f(i,j)$ is a zero or a one[2]. Then the two dimensional BIFORE transform (2-BT) of the data matrix $\underline{f}(x_1,x_2)$ in (3-1) is defined as

$$F(u_1,u_2) = \frac{1}{N_1N_2} \sum_{x_1=0}^{N_1-1} \sum_{x_2=0}^{N_2-1} f(x_1,x_2)(-1)^{\langle x,u\rangle} \qquad (3\text{-}2)$$

---

1. Note that N_1 need not be equal to N_2

2. In general $f(i,j)$ can be any finite real number

where

$F(u_1,u_2)$ is a transform coefficient

$f(x_1,x_2)$ is an input data point

$$u_i = 0,1,\ldots,(N_i-1);i=1,2 \tag{3-3}$$

$$<x_i,u_i>= \sum_{m=0}^{n_i-1} u_i(m)x_i(m)$$

$$<x,u> = <x_1,u_1> + <x_2,u_2>$$

and

$$n_i = \log_2 N_i, i=1,2.$$

The terms $u_i(m)$ and $x_i(m)$ in (3-3) are the binary representations of u_i and x_i respectively. For example,

$$[u_i]_{decimal} = [u_i(k_i-1),\ u_i(k_i-2),\ldots,\ u_i\ (1),\ u_i(0)]_{binary} \tag{3-4}$$

where

$$u_i\ (\ ) \in \{0,1\}.$$

Alternately, (3-2) can be written in the form of a matrix to obtain

$$\left[\underline{F}(u_1,u_2)\right] = \frac{1}{N_1N_2} \left[H(n_1)\right] \left[\underline{f}(x_1,x_2)\right] \left[H(n_2)\right] \tag{3-5}$$

where

$\left[\underline{F}(u_1,u_2)\right]$ is a $(N_1 x N_2)$ transform matrix corresponding to the data matrix $\left[\underline{f}(x_1,x_2)\right]$

$\left[H(n_1)\right]$ and $\left[H(n_2)\right]$ are $(N_1 x N_1)$ and $(N_2 x N_2)$ Hadamard matrices with $n_i = \log_2 N_i$, $i=1, 2$.

The Hadamard matrices in (3-5) are defined by the recurrence relation

$$H(k+1) = \left[\begin{array}{c|c} H(k) & H(k) \\ \hline H(k) & -H(k) \end{array}\right] \qquad k=0,1,\ldots,n_i \tag{3-6}$$

$$H(0) = 1$$

From (3-6) it follows that the elements of a Hadamard matrix are either +1 or -1.

Using the fact that the 2-BT is an orthogonal transform, it can be shown that (3-7) the corresponding inverse transform (2-IBT) is defined as

$$f(x_1,x_2) = \sum_{u_1=0}^{N_1-1} \sum_{u_2=0}^{N_2-1} F(u_1,u_2)\,(-1)^{<x,u>} \qquad (3\text{-}7)$$

or alternately as

$$\left[\underline{f}(x_1,x_2)\right] = \left[H(n_1)\right]\left[\underline{F}(u_1,u_2)\right]\left[H(n_2)\right] \qquad (3\text{-}8)$$

3.2 The 2-BT Power Spectrum

A BIFORE power spectrum which is analogous to a two-dimensional Fourier power spectrum can be defined as

$$P(z_1,z_2) = \sum_{u_1=\left[2^{z_1-1}\right]}^{2^{z_1}-1} \sum_{u_2=\left[2^{z_2-1}\right]}^{2^{z_2}-1} F^2(u_1,u_2) \qquad (3\text{-}9)$$

where

$z_i=0,\ 1,\ \ldots,\ k_i;\ n_i = \log_2 N_i,\quad i=1,2.$

and

$\left[2^{z_i-1}\right]$ is the integer part of 2^{z_i-1}.

From (3-9) it follows that the 2-BT power spectrum can be expressed in matrix form to obtain

$$\left[\underline{P}(k_1,k_2)\right] = \begin{bmatrix} P(0,0) & P(0,1) & \ldots & P(0,n_2) \\ P(1,0) & P(1,1) & \ldots & P(1,n_2) \\ & \ldots & & \\ P(n_1,0) & P(n_1,1) & \ldots & P(n_1,n_2) \end{bmatrix} \qquad (3\text{-}10)$$

Inspection of (3-10) reveals that the number of 2-BT power spectrum points is given by

$$\Sigma = (1+n_1)\ (1+n_2); \quad n_i = \log_2 N_i,\ i=1,2 \qquad (3\text{-}11)$$

In this study, we attempt to characterize the <u>size</u> and <u>shape</u> of grain kernels by the $(1+\log_2 N_1)\ (1+\log_2 N_2)$ power spectrum points given by the matrix$\left[\underline{P}(k_1,k_2)\right]$in (3-10). The motivation for this choice of the power spectrum will be considered in Section 3-4.

3.3 A Numerical Example

A numerical example will be helpful to clarify the discussion made above. Suppose the 2-BT power spectrum of the pattern shown in Figure 3-1 are desired.

0	0	0	0	0	0	0	0
0	0	0	1	1	0	0	0
0	0	1	1	1	1	0	0
0	0	1	1	1	1	0	0
0	0	1	1	1	1	0	0
0	0	0	1	1	0	0	0
0	0	0	0	0	0	0	0
0	0	0	0	0	0	0	0

Figure 3-1. An (8x8) pattern

From Figure 3-1 it follows that $N_1=N_2=8$. Thus (3-5) yields

$$\left[\underline{F}(u_1,u_2)\right] = \frac{1}{64}\left[H(3)\right]\left[\underline{f}(x_1,x_2)\right]\left[H(3)\right] \tag{3-12}$$

Using (3-6) to evaluate $\left[H(3)\right]$ and subsequently substituting in (3-12) there results the following matrix equation.

$$\left[\underline{F}(u_1,u_2)\right] = \frac{1}{64}\left[H(3)\right]\begin{bmatrix} 0&0&0&0&0&0&0&0\\ 0&0&0&1&1&0&0&0\\ 0&0&1&1&1&1&0&0\\ 0&0&1&1&1&1&0&0\\ 0&0&1&1&1&1&0&0\\ 0&0&0&1&1&0&0&0\\ 0&0&0&0&0&0&0&0\\ 0&0&0&0&0&0&0&0 \end{bmatrix}\left[H(3)\right] \tag{3-13}$$

where

$$\left[H(3)\right] = \left[\begin{array}{cccc|cccc} 1&1&1&1&1&1&1&1\\ 1&-1&1&-1&1&-1&1&-1\\ 1&1&-1&-1&1&1&-1&-1\\ 1&-1&-1&1&1&-1&-1&1\\ \hline 1&1&1&1&-1&-1&-1&-1\\ 1&-1&1&-1&-1&1&-1&1\\ 1&1&-1&-1&-1&-1&1&1\\ 1&-1&-1&1&-1&1&1&-1 \end{array}\right] \tag{3-14}$$

Evaluation of (3-13) yields the transform matrix

$$\left[\underline{F}(u_1,u_2)\right] = \frac{1}{64}\begin{bmatrix} 16 & 0 & 0 & 4 & 0 & -4 & -16 & 0 \\ 0 & 0 & 0 & -4 & 0 & 4 & 0 & 0 \\ 0 & 0 & 0 & 4 & 0 & -4 & 0 & 0 \\ 0 & 0 & 0 & -4 & 0 & 4 & 0 & 0 \\ 4 & 0 & 0 & 0 & 0 & 0 & -4 & 0 \\ -4 & 0 & 0 & 0 & 0 & 0 & 4 & 0 \\ 12 & 0 & 0 & 0 & 0 & 0 & -12 & 0 \\ -4 & 0 & 0 & 0 & 0 & 0 & 4 & 0 \end{bmatrix} \quad (3\text{-}15)$$

Substitution of the values of $F(u_1,u_2)$ obtained from (3-15) into (3-9) results in the following 2-BT power spectrum in matrix form.

$$\left[P(k_1,k_2)\right] = \frac{1}{256}\begin{bmatrix} 16 & 0 & 1 & 17 \\ 0 & 0 & 1 & 1 \\ 0 & 0 & 2 & 2 \\ 12 & 0 & 0 & 12 \end{bmatrix} \quad (3\text{-}16)$$

3.4 Motivation for Using the 2-BT Power Spectrum.

We attempt to characterize the size and shape of grain kernels by the $(1+\log_2 N_1)$ $(1+\log_2 N_2)$ power spectrum points given by the matrix $\left[\underline{P}(k_1,k_2)\right]$ in (3-10). Three reasons can be quoted for doing so.

(1). The power spectrum represents the distribution of power in a given two-dimensional pattern. This is best illustrated by a simple example with $N_1=2, N_2=4$ and

$$\left[\underline{f}(x_1,x_2)\right] = \begin{bmatrix} 3 & 0 & 3 & 4 \\ 3 & 8 & 7 & 8 \end{bmatrix} \quad (3\text{-}17)$$

Applying (3-5) and (3-9) to (3-12) results in the following 2-BT power spectrum

$$P(0,0) = 81/4, \quad P(0,1) = 1/4, \quad P(0,2) = 1$$
$$P(1,0) = 4, \quad P(1,1) = 1, \quad P(1,2) = 1 \tag{3-18}$$

Now, it can be shown that $\left[\underline{f}(x_1,x_2)\right]$ in (3-17) can be decomposed into the following <u>mutually orthogonal</u> sub-patterns:

$$\left[\underline{f}_{00}(x_1,x_2)\right] = \begin{bmatrix} 4.5 & 4.5 & 4.5 & 4.5 \\ 4.5 & 4.5 & 4.5 & 4.5 \end{bmatrix}$$

$$\left[\underline{f}_{01}(x_1,x_2)\right] = \begin{bmatrix} -0.5 & 0.5 & -0.5 & 0.5 \\ -0.5 & 0.5 & -0.5 & 0.5 \end{bmatrix}$$

$$\left[\underline{f}_{02}(x_1,x_2)\right] = \begin{bmatrix} -1 & -1 & 1 & 1 \\ -1 & -1 & 1 & 1 \end{bmatrix}$$

$$\left[\underline{f}_{10}(x_1,x_2)\right] = \begin{bmatrix} -2 & -2 & -2 & -2 \\ 2 & 2 & 2 & 2 \end{bmatrix} \tag{3-19}$$

$$\left[\underline{f}_{11}(x_1,x_2)\right] = \begin{bmatrix} 1 & -1 & 1 & -1 \\ -1 & 1 & -1 & 1 \end{bmatrix}$$

and

$$\left[\underline{f}_{12}(x_1,x_2)\right] = \begin{bmatrix} 1 & -1 & -1 & 1 \\ -1 & 1 & 1 & -1 \end{bmatrix}$$

It is straight forward to verify that

$$\underline{f}(x_1,x_2) = \sum_{i=0}^{2}\left[\underline{f}_{0i}(x_1,x_2)\right] + \sum_{i=0}^{2}\left[\underline{f}_{1i}(x_1,x_2)\right] \tag{3-20}$$

Inspection of the sub-patterns in (3-19) reveals that $\left[\underline{f}_{ij}(x_1,x_2)\right]$ is 2^i - periodic with respect to the first dimension (i.e. the columns) and

2^j - periodic in the second dimension (i.e. the rows). If $\sum_{i,j} \left[\underline{f}_{ij}(x_1,x_2)\right]^2$ denotes the sum of the squares of the elements in the sub-pattern $\left[\underline{f}_{i,j}(x_1,x_2)\right]$, divided by N_1N_2, then it can be verified that

$$\sum_{i,j} \left[\underline{f}_{00}(x_1,x_2)\right]^2 = 81/4 \qquad \sum_{i,j} \left[\underline{f}_{01}(x_1,x_2)\right]^2 = 1/4$$

$$\sum_{i,j} \left[\underline{f}_{02}(x_1,x_2)\right]^2 = 1 \qquad \sum_{i,j} \left[\underline{f}_{10}(x_1,x_2)\right]^2 = 4 \tag{3-21}$$

$$\sum_{i,j} \left[\underline{f}_{11}(x_1,x_2)\right]^2 = 1 \qquad \sum_{i,j} \left[\underline{f}_{12}(x_1,x_2)\right]^2 = 1$$

Comparing (3-18) and (3-21) it is clear that each of the 2-BT power spectrum points represents the average power in one of the mutually orthagonal sub-patterns $\left[\underline{f}_{ij}(x_1,x_2)\right]$. Thus the 2-BT power spectrum represents the distribution of power in a given two-dimensional pattern. In the problem at hand, such two-dimensional patterns are coded images (see Figure 1-3) which characterize the sizes and shapes of grain kernels.

(2). From the periodicities present in the sub-patterns $\left[\underline{f}_{ij}(x_1,x_2)\right]$, the analogy between the 2-BT power spectrum and the familiar discrete Fourier power spectrum is apparent. Again, the property that the Fourier power spectrum is invariant with respect to cyclic shifts without rotation of a pattern as illustrated in Figure 3-2 is also valid for the BIFORE spectrum. However, the 2-BT power spectrum yields considerable data compression since it consists of $(1+\log_2 N_1)(1+\log_2 N_2)$ spectrum points in contrast to $(N_1/2+1)(N_2/2+1)$ independent discrete Fourier spectrum points.

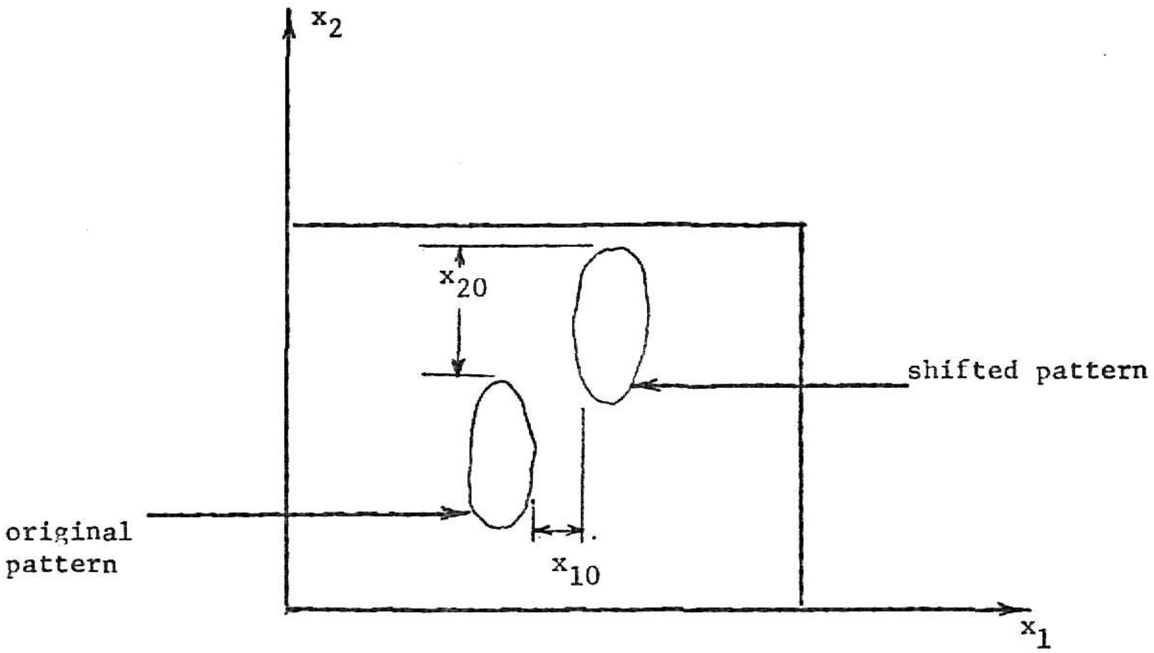

Figure 3-2 Illustration of the shift-invariance property.

(3). The 2-BT power spectrum can be computed rapidly using an algorithm called the fast BIFORE transform (FBT). The corresponding computer program is included in Appendix 4-1. Since only real arithmetic operations are involved, the corresponding implementation is simpler relative to that of the Fourier spectrum which requires complex arithmetic operations.

CHAPTER IV

EXPERIMENTAL RESULTS

4.1 Data Collection

A block diagram of the set up used to obtain the data is shown in Figure 4-1. Each kernel was placed at the base of a microfilm reader and projected on its screen. A (32x32) grid was attached to the screen for each kernel. Each square of the grid which was occupied by the kernel image was coded by a '1' and by a '0' otherwise. A typical output obtained from this stage of the data processing is shown in Figure 4-2. Before any such data was taken, the microfilm reader was calibrated each time using a standard circular pattern which is shown in Figure 4-3. The image coded pattern corresponding to this calibration pattern is shown in Figure 4-4.

The above output of the film reader in the form of a (32x32) array of ones and zeros was punched IBM cards and used as data for the computer program listed in Appendix 4-1. This program was used to compute the 2-BT (BIFORE TRANSFORM) power spectra of several grain kernels placed in random orientations. The corresponding 2-BT power spectra that resulted were in the form of (6x6) matrix i.e. 36 components. Twenty out of the 36 components whose magnitudes were relatively large were chosen. These are tabulated in Appendix 4-2. For convenience each spectrum point in this table has been multiplied by a scale factor of 10^3.

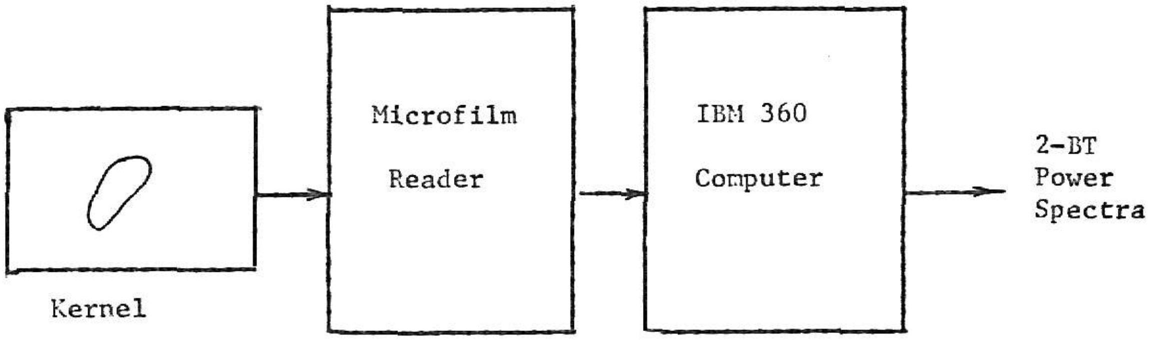

Figure 4-1. Block diagrm of set up to gather data

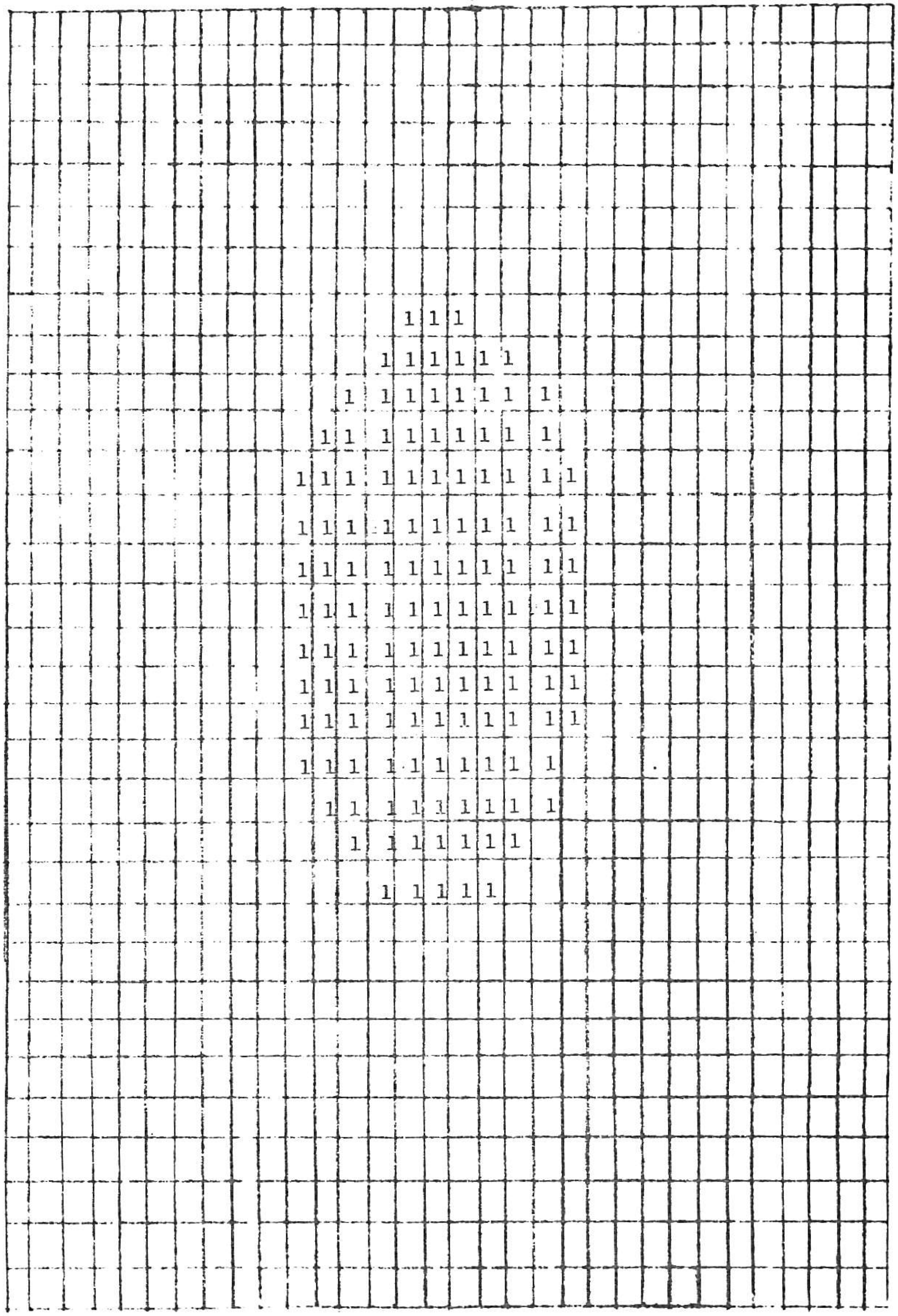

Figure 4-2. Typical output from microfilm reader.

(Blank elements of the array consist of zeros).